Supplemental Material for Stability of Bogoliubov Fermi Surfaces within BCS Theory

Ankita Bhattacharya and Carsten Timm

I. BASIS MATRICES AND DETAILS OF THE MODEL

In this section, we summarize the basis matrices that appear in both the normal-state Hamiltonian $H_N(\mathbf{k})$ and in the superconducting pairing matrix $\hat{\Delta}$. We also present details of the model Hamiltonian. In terms of the standard spin-3/2 matrices

$$J_x = \frac{1}{2}\begin{pmatrix} 0 & \sqrt{3} & 0 & 0 \\ \sqrt{3} & 0 & 2 & 0 \\ 0 & 2 & 0 & \sqrt{3} \\ 0 & 0 & \sqrt{3} & 0 \end{pmatrix}, \tag{S1}$$

$$J_y = \frac{i}{2}\begin{pmatrix} 0 & -\sqrt{3} & 0 & 0 \\ \sqrt{3} & 0 & -2 & 0 \\ 0 & 2 & 0 & -\sqrt{3} \\ 0 & 0 & \sqrt{3} & 0 \end{pmatrix}, \tag{S2}$$

$$J_z = \frac{1}{2}\begin{pmatrix} 3 & 0 & 0 & 0 \\ 0 & 1 & 0 & 0 \\ 0 & 0 & -1 & 0 \\ 0 & 0 & 0 & -3 \end{pmatrix}, \tag{S3}$$

the basis matrices are given by [1–3]

$$h_0 = \mathbb{1}, \tag{S4}$$

$$h_1 = \frac{J_yJ_z + J_zJ_y}{\sqrt{3}}, \tag{S5}$$

$$h_2 = \frac{J_zJ_x + J_xJ_z}{\sqrt{3}}, \tag{S6}$$

$$h_3 = \frac{J_xJ_y + J_yJ_x}{\sqrt{3}}, \tag{S7}$$

$$h_4 = \frac{J_x^2 - J_y^2}{\sqrt{3}}, \tag{S8}$$

$$h_5 = \frac{2J_z^2 - J_x^2 - J_y^2}{3}, \tag{S9}$$

which are orthonormalized so that $\mathrm{Tr}\, h_m h_n = 4\delta_{mn}$. The matrices h_1 to h_5 transform under point-group operations like the basis functions yz, zx, xy, $x^2 - y^2$, and $3z^2 - r^2$. h_1 to h_3 are irreducible tensor operators belonging to the irrep T_{2g}, while h_4 and h_5 are irreducible tensor operators belonging to E_g.

The normal-state Hamiltonian can be expanded as

$$H_N(\mathbf{k}) = \sum_{n=0}^{5} c_n(\mathbf{k})\, h_n. \tag{S10}$$

Under point-group operations, the functions $c_n(\mathbf{k})$ must transform in the same way as the h_n so that the full Hamiltonian transforms trivially. The $c_n(\mathbf{k})$ must also respect the periodicity of the reciprocal lattice. We assume a face-centered-cubic lattic, which is appropriate for example for an effective model of a pyrochlore [4] and for Heusler

compounds if antisymmetric spin-orbit coupling is negligible [5]. The functions $c_n(\mathbf{k})$ are chosen as

$$c_0(\mathbf{k}) = (-4t_1 - 5t_2)(\cos k_x \cos k_y + \cos k_y \cos k_z + \cos k_z \cos k_x) - \mu, \tag{S11}$$
$$c_1(\mathbf{k}) = 4\sqrt{3}\, t_3 \sin k_y \sin k_z, \tag{S12}$$
$$c_2(\mathbf{k}) = 4\sqrt{3}\, t_3 \sin k_z \sin k_x, \tag{S13}$$
$$c_3(\mathbf{k}) = 4\sqrt{3}\, t_3 \sin k_x \sin k_y, \tag{S14}$$
$$c_4(\mathbf{k}) = -2\sqrt{3}\, t_2(\cos k_y \cos k_z - \cos k_z \cos k_y), \tag{S15}$$
$$c_5(\mathbf{k}) = 2t_2(\cos k_y \cos k_z + \cos k_z \cos k_x - 2\cos k_x \cos k_y). \tag{S16}$$

Including higher-order trigonometric functions, corresponding to longer-range hopping in real space, would not affect the qualitative results. For the numerical calculations, we set $t_1 = -0.918\,\mathrm{eV}$, $t_2 = -0.760\,\mathrm{eV}$, $t_3 = -0.253\,\mathrm{eV}$, and $\mu = -0.88\,\mathrm{eV}$. These values originally come from a tight-binding fit to density-functional results for the band structure of the half-Heusler compound YPtBi, neglecting the inversion-symmetry-breaking antisymmetric spin-orbit coupling, see Ref. [5].

II. ANALYTICAL EXPRESSIONS

In the following, we present the secular equations for the eigenenergies of the BdG Hamiltonian. We also give useful closed expressions for the coefficients of these equations and for derivatives of eigenenergies with respect to the pairing amplitudes.

A. Closed form of eigenenergies

The eigenvalues of the BdG Hamiltonian

$$\mathcal{H}(\mathbf{k}) = \begin{pmatrix} H_N(\mathbf{k}) & \hat{\Delta} \\ \hat{\Delta}^\dagger & -H_N^T(-\mathbf{k}) \end{pmatrix} \tag{S17}$$

can be obtained in analytical form. The secular equation for eigenvalues E of $\mathcal{H}$ is of order eight but the presence of both inversion symmetry and charge-conjugation symmetry guarantees that the solutions come in pairs of opposite sign. This allows us to reduce the secular equation to two quartic equations

$$E^4 + pE^2 \pm qE + r = 0. \tag{S18}$$

It is sufficient to solve one of them since the solutions of the other one are simply the negative of the solutions of the first. We consider the first one,

$$E^4 + pE^2 + qE + r = 0. \tag{S19}$$

Since the equation is of depressed form (there is no E^3 term) the solutions satisfy $E_1 + E_2 + E_3 + E_4 = 0$. To give the analytical expressions for the coefficients p, q, and r, we define the five-component vectors

$$\vec{c} \equiv (c_1, c_2, c_3, c_4, c_5), \tag{S20}$$
$$\vec{\Delta}^1 \equiv (\Delta_1^1, \Delta_2^1, \Delta_3^1, \Delta_4^1, \Delta_5^1), \tag{S21}$$
$$\vec{\Delta}^2 \equiv (\Delta_1^2, \Delta_2^2, \Delta_3^2, \Delta_4^2, \Delta_5^2). \tag{S22}$$

In Eq. (S20), we have suppressed the momentum argument. We further define the Gram matrix of these vectors [6],

$$M \equiv \begin{pmatrix} \vec{c}\cdot\vec{c} & \vec{c}\cdot\vec{\Delta}^1 & \vec{c}\cdot\vec{\Delta}^2 \\ \vec{\Delta}^1\cdot\vec{c} & \vec{\Delta}^1\cdot\vec{\Delta}^1 & \vec{\Delta}^1\cdot\vec{\Delta}^2 \\ \vec{\Delta}^2\cdot\vec{c} & \vec{\Delta}^2\cdot\vec{\Delta}^1 & \vec{\Delta}^2\cdot\vec{\Delta}^2 \end{pmatrix}. \tag{S23}$$

Being a Gram matrix, M is real and symmetric and also positive semidefinite. The following expressions have been derived with the help of Mathematica [7], making use of the SO(5) invariance of the eigenenergies under simultaneous

rotations of the vectors $\vec{c}$, $\vec{\Delta}^1$, and $\vec{\Delta}^2$, which follows from the expansion of $\mathcal{H}(\mathbf{k})$ into 18 basis matrices and their commutation relations described in Ref. [8].

The first coefficient p reads as

$$p = -2\left[\sum_{n=0}^{5} c_n^2 + \sum_{n=0}^{5}(\Delta_n^1)^2 + \sum_{n=0}^{5}(\Delta_n^2)^2\right] = -2\left[c_0^2 + (\Delta_0^1)^2 + (\Delta_0^2)^2\right] - 2\ \mathrm{Tr}\ M. \tag{S24}$$

This coefficient is clearly nonzero and negative whenever $\mathcal{H}$ is not the null matrix. The characteristic energy scale of the BdG Hamiltonian is $\sqrt{-p/2}$.

The second coefficient q is more interesting. If q vanishes the quartic equations (S18) become biquadratic and have the solutions E_1, $-E_1$, E_2, $-E_2$. Since the two quartic equations become identical all eigenenergies are at least twofold degenerate. Since they must be twofold degenerate in the presence of inversion symmetry and TRS by the Kramers theorem these symmetries imply $q = 0$. The reverse statement does not hold. The coefficient q is given by

$$\begin{aligned} q = 8\sqrt{\det M} = 8\Big[&(\vec{c}\cdot\vec{c})(\vec{\Delta}^1\cdot\vec{\Delta}^1)(\vec{\Delta}^2\cdot\vec{\Delta}^2)] + 2(\vec{c}\cdot\vec{\Delta}^1)(\vec{\Delta}^1\cdot\vec{\Delta}^2)(\vec{\Delta}^2\cdot\vec{c}) - (\vec{c}\cdot\vec{c})(\vec{\Delta}^1\cdot\vec{\Delta}^2)^2 \\ &- (\vec{\Delta}^1\cdot\vec{\Delta}^1)(\vec{\Delta}^2\cdot\vec{c})^2 - (\vec{\Delta}^2\cdot\vec{\Delta}^2)(\vec{c}\cdot\vec{\Delta}^1)^2\Big]^{1/2}. \end{aligned} \tag{S25}$$

Nonzero q implies a nonzero Gram matrix M and thus that the three five-component vectors $\vec{c}$, $\vec{\Delta}^1$, and $\vec{\Delta}^2$ are linearly independent. Therefore, twofold degeneracy of the eigenvalues requires $\vec{c}$, $\vec{\Delta}^1$, and $\vec{\Delta}^2$ to be coplanar (or zero). We note that q does not depend on the "singlet" components c_0, Δ_0^1, and Δ_0^2.

Using the generalized "Minkowski" product

$$\langle A, B\rangle \equiv A_0 B_0 - \vec{A}\cdot\vec{B}, \tag{S26}$$

the third coefficient r can be written as

$$\begin{aligned} r = &\langle c,c\rangle^2 + \langle\Delta^1,\Delta^1\rangle^2 + \langle\Delta^2,\Delta^2\rangle^2 + 4\left(\langle c,\Delta^1\rangle^2 + \langle\Delta^1,\Delta^2\rangle^2 + \langle\Delta^2,c\rangle^2\right) \\ &- 2\left(\langle c,c\rangle\langle\Delta^1,\Delta^1\rangle + \langle\Delta^1,\Delta^1\rangle\langle\Delta^2,\Delta^2\rangle + \langle\Delta^2,\Delta^2\rangle\langle c,c\rangle\right). \end{aligned} \tag{S27}$$

To get insight into the significance of r, we use the Vieta theorem to rewrite the polynomial in Eq. (S19) as

$$E^4 + pE^2 + qE + r = (E - E_1)(E - E_2)(E - E_3)(E - E_4), \tag{S28}$$

where E_i are the solutions of the quartic equation. Setting $E = 0$ we obtain

$$r = E_1 E_2 E_3 E_4. \tag{S29}$$

Note that $\det\mathcal{H} = E_1^2 E_2^2 E_3^2 E_4^2 = r^2$ is the square of the Pfaffian $P(\mathbf{k})$ of the BdG Hamiltonian unitarily transformed into antisymmetric form. The Pfaffian determines the $\mathbb{Z}_2$ invariant that protects BFSs in centrosymmetric superconductors [1, 3]. Obviously, nodes of any type, including BFSs, are characterized by zeros of $\det\mathcal{H}$ and thus by zeros of the Pfaffian. At BFSs specifically, the Pfaffian generically changes sign as a function of momentum $\mathbf{k}$. We find that r equals the Pfaffian $P(\mathbf{k})$, up to the sign. However, the overall sign of the Pfaffian is not unitarily invariant and therefore not physically meaningful [1, 3]. We can thus choose this sign in such a way that $r = P(\mathbf{k})$.

Equation (S27) can be rewritten as

$$r = \left(\langle c,c\rangle - \langle\Delta^1,\Delta^1\rangle - \langle\Delta^2,\Delta^2\rangle\right)^2 + 4\left(\langle c,\Delta^1\rangle^2 + \langle\Delta^1,\Delta^2\rangle^2 + \langle\Delta^2,c\rangle^2 - \langle\Delta^1,\Delta^1\rangle\langle\Delta^2,\Delta^2\rangle\right). \tag{S30}$$

We observe that the first term is a complete square. Hence, the Pfaffian $r = P(\mathbf{k})$ can only change sign when both $\vec{\Delta}^1$ and $\vec{\Delta}^2$ have at least one nonzero component.

With the values of p, q, and r at hand, the solutions of the quartic equation can be obtained in closed form using the Ferrari-Cardano method. However, it turns out to be numerically more robust to obtain them as the eigenvalues of the companion matrix [6]

$$C = \begin{pmatrix} 0 & 0 & 0 & -r \\ 1 & 0 & 0 & -q \\ 0 & 1 & 0 & -p \\ 0 & 0 & 1 & 0 \end{pmatrix}.$$

B. Derivatives of eigenenergies

The BCS gap equation (8) in the main text, as well as the inverse gap equation (9), contain derivatives of eigenenergies with respect to the pairing amplitudes Δ_n^α. For high-precision results, it is beneficial to evaluate these derivatives analytically instead of numerically using a finite-difference formula. Noting that the eigenenergies are solutions of the quartic equations $E^4 + pE^2 + qE + r = 0$, the derivatives $\partial E_{\mathbf{k},i}/\partial\Delta_n^\alpha$ can be expressed in terms of derivatives of the coefficients p, q, and r:

$$\frac{\partial E}{\partial \Delta_n^\alpha} = \frac{\partial E}{\partial p}\frac{\partial p}{\partial \Delta_n^\alpha} + \frac{\partial E}{\partial q}\frac{\partial q}{\partial \Delta_n^\alpha} + \frac{\partial E}{\partial r}\frac{\partial r}{\partial \Delta_n^\alpha}, \tag{S31}$$

where

$$\frac{\partial E}{\partial p} = -\frac{E^2}{4E^3 + 2pE + q}, \tag{S32}$$

$$\frac{\partial E}{\partial q} = -\frac{E}{4E^3 + 2pE + q}, \tag{S33}$$

$$\frac{\partial E}{\partial r} = -\frac{1}{4E^3 + 2pE + q}. \tag{S34}$$

Inserting these equations into Eq. (S31) yields

$$\frac{\partial E}{\partial \Delta_n^\alpha} = -\frac{1}{4E^3 + 2pE + q}\left(E^2\frac{\partial p}{\partial \Delta_n^\alpha} + E\frac{\partial q}{\partial \Delta_n^\alpha} + \frac{\partial r}{\partial \Delta_n^\alpha}\right). \tag{S35}$$

The closed expressions for the coefficients p, q, and r derived above allow us to write down the derivatives with respect to Δ_n^α. To start with, Eq. (S24) simply gives

$$\frac{\partial p}{\partial \Delta_n^\alpha} = -4\Delta_n^\alpha. \tag{S36}$$

If $q \neq 0$ we can write

$$\frac{\partial q}{\partial \Delta_n^\alpha} = \frac{1}{2q}\frac{\partial q^2}{\partial \Delta_n^\alpha}. \tag{S37}$$

Equation (S26) shows that q does not depend on Δ_0^α. Thus, we obtain $\partial q^2/\partial\Delta_0^\alpha = 0$ and

$$\begin{aligned}
\frac{\partial q^2}{\partial \Delta_n^\alpha} &= 64\,\frac{\partial}{\partial \Delta_n^\alpha}\,\det M \\
&= 128\Big\{(\vec{c}\cdot\vec{c})(\vec{\Delta}^{\bar\alpha}\cdot\vec{\Delta}^{\bar\alpha})\,\Delta_n^\alpha + (\vec{c}\cdot\vec{\Delta}^{\bar\alpha})(\vec{\Delta}^1\cdot\vec{\Delta}^2)\,c_n + (\vec{c}\cdot\vec{\Delta}^1)(\vec{c}\cdot\vec{\Delta}^2)\,\Delta_n^{\bar\alpha} - (\vec{c}\cdot\vec{\Delta}^{\bar\alpha})^2\,\Delta_n^\alpha \\
&\quad - (\vec{c}\cdot\vec{c})(\vec{\Delta}^1\cdot\vec{\Delta}^2)\,\Delta_n^{\bar\alpha} - (\vec{c}\cdot\vec{\Delta}^\alpha)(\vec{\Delta}^{\bar\alpha}\cdot\vec{\Delta}^{\bar\alpha})\,c_n\Big\} \\
&= 128\Big\{\left[(\vec{c}\cdot\vec{\Delta}^{\bar\alpha})(\vec{\Delta}^1\cdot\vec{\Delta}^2) - (\vec{c}\cdot\vec{\Delta}^\alpha)(\vec{\Delta}^{\bar\alpha}\cdot\vec{\Delta}^{\bar\alpha})\right]c_n + \left[(\vec{c}\cdot\vec{c})(\vec{\Delta}^{\bar\alpha}\cdot\vec{\Delta}^{\bar\alpha}) - (\vec{c}\cdot\vec{\Delta}^{\bar\alpha})^2\right]\Delta_n^\alpha \\
&\quad + \left[(\vec{c}\cdot\vec{\Delta}^1)(\vec{c}\cdot\vec{\Delta}^2) - (\vec{c}\cdot\vec{c})(\vec{\Delta}^1\cdot\vec{\Delta}^2)\right]\Delta_n^{\bar\alpha}\Big\}
\end{aligned} \tag{S38}$$

for $n \geq 1$, where $\bar\alpha = 2$ (1) for $\alpha = 1$ (2).

Finally, from Eq. (S27), we obtain

$$\begin{aligned}
\frac{\partial r}{\partial \Delta_n^\alpha} &= 4s_n\langle\Delta^\alpha,\Delta^\alpha\rangle\,\Delta_n^\alpha + 8s_n\langle c,\Delta^\alpha\rangle\,c_n + 8s_n\langle\Delta^1,\Delta^2\rangle\,\Delta_n^{\bar\alpha} - 4s_n\langle c,c\rangle\,\Delta_n^\alpha - 4s_n\langle\Delta^{\bar\alpha},\Delta^{\bar\alpha}\rangle\,\Delta_n^\alpha \\
&= 4s_n\left[2\langle c,\Delta^\alpha\rangle\,c_n + \left(\langle\Delta^\alpha,\Delta^\alpha\rangle - \langle\Delta^{\bar\alpha},\Delta^{\bar\alpha}\rangle - \langle c,c\rangle\right)\Delta_n^\alpha + 2\langle\Delta^1,\Delta^2\rangle\,\Delta_n^{\bar\alpha}\right],
\end{aligned} \tag{S39}$$

where $s_n = 1$ (-1) for $n = 0$ $(n \geq 1)$. This concludes the derivation of the explicit form of the derivatives appearing in the gap equation. The results show explicitly that all the derivatives are at least of first order in Δ_n^α, which has been used in the derivation of the inverse gap equation in the main text.

III. WEAK-COUPLING SCALING

In this section, we briefly review the scaling of the pairing amplitude Δ and the free (internal) energy with the interaction strength at temperature $T = 0$. By performing the momentum integration in Eq. (6) in the main text and expanding up to order Δ^2, we obtain the free-energy difference per unit cell as

$$\Delta F = F_s - F_n \cong c_1 \Delta^2 \ln \Delta + c_2 \Delta^2 + \frac{1}{2}\frac{\Delta^2}{V} = \left(c_1 \ln \Delta + c_2 + \frac{1}{2V} \right) \Delta^2, \tag{S40}$$

where c_1 and c_2 are coefficients and V is the interaction strength, see Eq. (7) in the main text. The last term stems from the mean-field decoupling in the Cooper channel. The expansion of the momentum sum for small Δ generates a leading term proportional to $\Delta^2 \ln \Delta$ (the Cooper logarithm), another contribution of order Δ^2, and terms of orders higher than Δ^2, which are omitted here. A normalizing factor inside the logarithm has been absorbed into c_2.

The saddle point is found by taking

$$0 \stackrel{!}{=} \frac{\partial \Delta F}{\partial \Delta} \cong c_1 \Delta + 2 \left(c_1 \ln \Delta + c_2 + \frac{1}{2V} \right) \Delta = \left(c_1 + 2c_2 + \frac{1}{V} + 2c_1 \ln \Delta \right) \Delta. \tag{S41}$$

For the nontrivial solution, we find

$$\ln \Delta \cong -\frac{1}{2} - \frac{c_2}{c_1} - \frac{1}{2c_1 V} \equiv A - \frac{B}{V}. \tag{S42}$$

This is the weak-coupling scaling form of the pairing amplitude used in the main text.

From Eq. (S42), we also obtain the well-known BCS weak-coupling form of the pairing amplitude,

$$\Delta \cong e^{-1/2 - c_2/c_1}\, e^{-1/2c_1 V} \tag{S43}$$

and thus

$$\Delta^2 \cong e^{-1 - 2c_2/c_1}\, e^{-1/c_1 V}. \tag{S44}$$

Insertion of Eqs. (S42) and (S44) into Eq. (S40) gives the free energy difference at the saddle point,

$$\Delta F \cong -\frac{c_1}{2}\, e^{-1 - 2c_2/c_1}\, e^{-1/c_1 V}. \tag{S45}$$

We obtain the scaling form

$$\ln(-\Delta F) \cong \ln \frac{c_1}{2} - 1 - \frac{2c_2}{c_1} - \frac{1}{c_1 V} \equiv A' - \frac{B'}{V}. \tag{S46}$$

The coefficients in Eqs. (S42) and (S46) are related by

$$A' = \ln \frac{c_1}{2} - 1 - \frac{2c_2}{c_1} = 2A + \ln \frac{c_1}{2} = 2A - \ln 4B, \tag{S47}$$

$$B' = \frac{1}{c_1} = 2B. \tag{S48}$$

IV. NUMERICAL SOLUTION OF THE INVERSE GAP EQUATION

In this section, we provide some background for the numerical solution of the inverse gap equation. Both the free (internal) energy and the inverse gap equation contain integrations over the three-dimensional Brillouin zone. High precision in these integrations is essential for reaching the weak-coupling regime. Of course, symmetries can be exploited to restrict the integrals to a part of the Brillouin zone but it remains a three-dimensional integral for any lattice model.

The integration is particularly demanding with regard to precision because the weak-coupling behavior relies on a logarithmic term proportional to $\Delta^2 \ln(\Delta/\Lambda)$ in the free (internal) energy at $T = 0$, which has to be separated from a Δ^2 contribution, where both are exponentially small for weak pairing interaction. Here, Λ is a high-energy cutoff

resulting from the finite band width. The Cooper logarithm $\ln(\Delta/\Lambda)$ results from integration over the entire Brillouin zone, as shown by the presence of both the low-energy scale Δ and the high-energy scale Λ.

We find that the common method of summing over a momentum-space mesh becomes forbiddingly slow for three-dimensional systems if reasonable accuracy is desired. Instead, we have obtained good results using adaptive integration. We perform the integration using spherical coordinates. The radial integration is performed first, inside the angular integrals. In order to capture the effect of the superconducting gap close to the normal-state Fermi momentum k_F, the radial integration is split into four parts over the intervals $[0, k_F - k_1]$, $[k_F - k_1, k_F]$, $[k_F, k_F + k_2]$, and $[k_F + k_2, k_{\mathrm{BZ}}(\theta, \phi)]$, where $k_{\mathrm{BZ}}(\theta, \phi)$ describes the surface of the Brillouin zone in the (θ, ϕ) direction. The widths of the regions, i.e., the values of k_1 and k_2, are proportional to the gap Δ at k_F and the constants of proportionality are determined so as to minimize the numerical noise. The integrals are performed using globally adaptive sampling as implemented in Mathematica [7] with the accuracy goal set to 18 digits and the maximum number of recursions set to 12 for the first and fourth interval and to 8 for the second and third interval. We also used globally adaptive sampling for the integration over θ and ϕ with the accuracy goal set to 18 digits and the maximum number of recursions set to 4.

The main diagnostics for the quality of the numerical integration are the following: The pairing interaction and the free-energy gain ΔF are smooth functions of the gap Δ—recall that we are solving the inverse gap equation. If we push the calculations to smaller Δ than presented here, we observe step-like behavior typical for round-off error. The results in the range of weak pairing interactions agree with the expected weak-coupling scaling of BCS theory, see Sec. III. Moreover, the scaling of the gap Δ and of the free-energy gain $\Delta F = F_s - F_n$ are consistent with each other.

V. T_{2g} PAIRING STATES

In this section, we briefly present results for the T_{2g} pairing states obtained by solving the inverse gap equation. The results are largely analogous to the E_g case. The T_{2g} states are characterized by a three-component order parameter $(\Delta_1, \Delta_2, \Delta_3) \equiv \Delta\, \boldsymbol{\delta}$ [3]. Landau analysis predicts that $\boldsymbol{\delta} = (1,0,0)$, $(1,1,1)/\sqrt{3}$, $(1,i,0)/\sqrt{2}$, and $(1,\omega,\omega^2)/\sqrt{3}$ as potentially stable [3, 9], where $\omega = e^{2\pi i/3}$. Similar to E_g pairing, the phase diagram contains a first-order transition from the TRSB $(1,i,0)$ state at weak coupling to the time-reversal-symmetric $(1,0,0)$ state at strong coupling, as shown in Fig. S1. Also like for E_g pairing, the pairing amplitude Δ and the free-energy gain ΔF exhibit weak-coupling scaling for small pairing strength V_T and the numerical method is robust far into the weak-coupling regime. For larger V_T, all states show the S shape for Δ and swallowtail for ΔF characteristic for a first-order transition.

For T_{2g} pairing, there are two TRSB states. Of these, the chiral $(1,i,0)$ state is weakly favored over the cyclic $(1,\omega,\omega^2)$ state at weak coupling, as shown in the inset of Fig. S1(b). Recall that the largest value corresponds to the stable state since the factor $1/\Delta F_{(1,i,0)}$ is negative. This result is surprising in view of the well-known arguments by Sigrist and Ueda [10]: For infinitesimal coupling, the $(1,i,0)$ state has a line node on the equator of the normal-state Fermi surface and two point nodes at the poles [1, 3]. The $(1,\omega,\omega^2)$ state instead has eight point nodes [3]. Hence, one would expect the DOS close to the Fermi energy to be lower for the latter state. However, the quasiparticle dispersion close to the point nodes for the $(1,\omega,\omega^2)$ state is rather shallow compared to the $(1,i,0)$ state for otherwise identical parameters. Evidently, this destabilizes the $(1,\omega,\omega^2)$ state also in the limit of infinitesimal coupling. The main insight here is that a TRSB state with a line node can be stabilized over a TRSB state that only has point nodes.

The TRSB T_{2g} states develop BFSs for increasing V_T, which destabilize them relative to the time-reversal-symmetric $(1,0,0)$ and $(1,1,1)$ states. Initially, the $(1,0,0)$ state is weakly favored, as shown in the main panel of Fig. S1(b). For larger V_T, the free-energy gains of the $(1,0,0)$ and $(1,1,1)$ states approach each other but $(1,0,0)$ seems to remain favored.

In this context, it is also worth pointing out that the T_{2g} pairing states require a significantly larger interaction strength than the E_g pairing states to be stabilized. This is clearly seen in Fig. 2 in the main text. Since the pairing strengths in the T_{2g} and E_g channels become equal in the spherical limit this suggests that the E_g states, in particular the weak-couping $(1,i)$ state, are favored for systems with small normal-state Fermi surface. A different scenario that favors E_g pairing over both T_{2g} and conventional A_{1g} pairing has been proposed in Ref. [4] for pyrochlore materials.

[1] D. F. Agterberg, P. M. R. Brydon, and C. Timm, Bogoliubov Fermi surfaces in Superconductors with Broken Time-Reversal Symmetry, Phys. Rev. Lett. **118**, 127001 (2017).

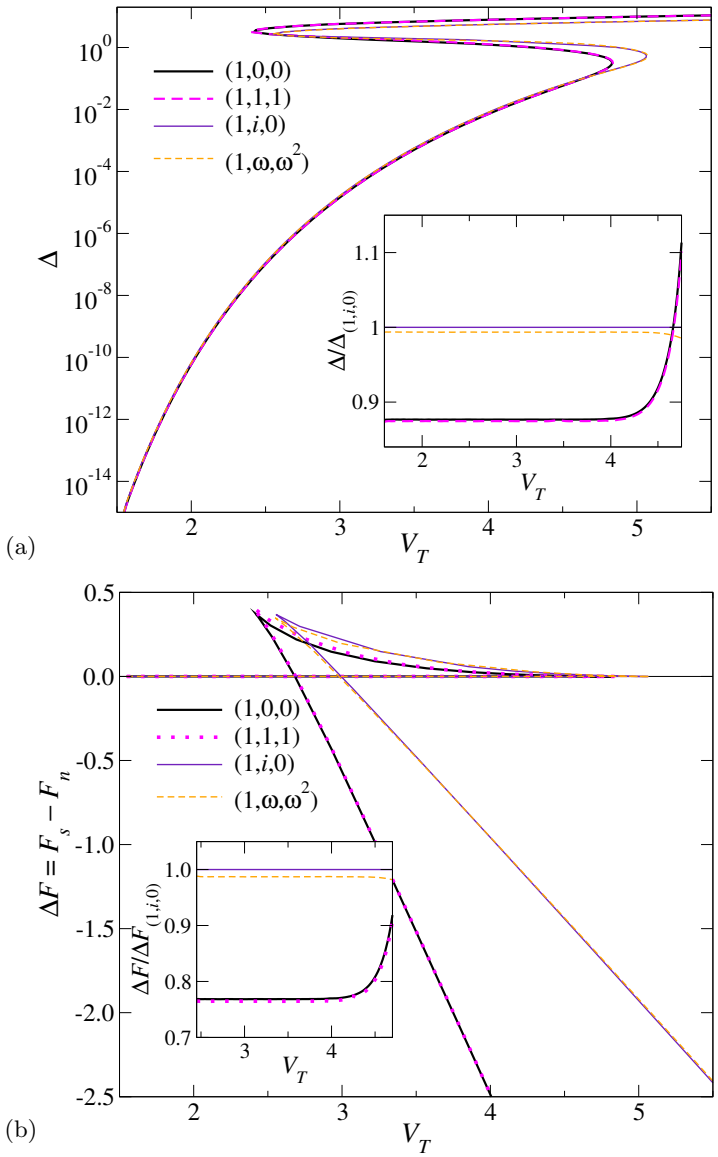

Figure S1. (a) Pairing amplitudes Δ as functions of the coupling strength V_T at $T = 0$ for the T_{2g} pairing states $(1, 0, 0)$, $(1, 1, 1)$, $(1, i, 0)$, and $(1, \omega, \omega^2)$ with $\omega = e^{2\pi i/3}$. The inset shows the ratios of Δ for the four states to Δ for the $(1, i, 0)$ state, which is the ground state at weak coupling. (b) Free-energy differences $\Delta F = F_s - F_n$ between the superconducting and normal states as functions of the coupling strength V_T at $T = 0$ for the same T_{2g} pairing states. The inset shows the ratios of ΔF for the three states to ΔF for the $(1, i)$ state. Details of the models and the numerical parameters are given in Sec. I.

[2] L. Savary, J. Ruhman, J. W. F. Venderbos, L. Fu, and P. A. Lee, Superconductivity in three-dimensional spin-orbit coupled semimetals, Phys. Rev. B **96**, 214514 (2017).

[3] P. M. R. Brydon, D. F. Agterberg, H. Menke, and C. Timm, Bogoliubov Fermi surfaces: General theory, magnetic order, and topology, Phys. Rev. B **98**, 224509 (2018).

[4] S. Kobayashi, A. Bhattacharya, C. Timm, and P. M. R. Brydon, Bogoliubov Fermi surfaces from pairing of emergent $j = \frac{3}{2}$ fermions on the pyrochlore lattice, Phys. Rev. B **105**, 134507 (2022).

[5] C. Timm, A. P. Schnyder, D. F. Agterberg, and P. M. R. Brydon, Inflated nodes and surface states in superconducting half-Heusler compounds, Phys. Rev. B **96**, 094526 (2017).

[6] R. A. Horn and C. R. Johnson, *Matrix Analysis* (Cambridge University Press, New York, 2012).

[7] Wolfram Research, Inc., Mathematica, Version 13.0, Champaign, IL (2021).

[8] C. Timm and A. Bhattacharya, Symmetry, nodal structures, and Bogoliubov Fermi surfaces for nonlocal pairing, Phys. Rev. B **104**, 094529 (2021).

[9] P. M. R. Brydon, L. M. Wang, M. Weinert, and D. F. Agterberg, Pairing of $j = 3/2$ Fermions in Half-Heusler Superconductors, Phys. Rev. Lett. **116**, 177001 (2016).

[10] M. Sigrist and K. Ueda, Phenomenological theory of unconventional superconductivity, Rev. Mod. Phys. **63**, 239 (1991).